AJNR

Activation of the sensorimotor cortex at 1.0 T: comparison of echo-planar and gradient-echo imaging.

B F van der Kallen, L J van Erning, M W van Zuijlen, H Merx and H O Thijssen

AJNR Am J Neuroradiol 1998, 19 (6) 1099-1104
http://www.ajnr.org/content/19/6/1099

AJNR Am J Neuroradiol 19:1099–1104, June 1998

Activation of the Sensorimotor Cortex at 1.0 T: Comparison of Echo-Planar and Gradient-Echo Imaging

Bas F. W. van der Kallen, Leon J. Th. O. van Erning, Mark W. J. van Zuijlen, Hans Merx, and Henk O. M. Thijssen

PURPOSE: **The increasing demand for the clinical application of functional MR imaging raises the question of whether this technique can be routinely performed on 1.0-T MR scanners. To this end, we assessed the feasibility of functional MR imaging at 1.0 T.**

METHODS: **Healthy volunteers were scanned during the performance of a motor task. Functional data were acquired with echo-planar imaging (EPI) and with gradient-echo (GRE) and dual-echo GRE sequences. The signal intensity variations of the EPI and GRE sequences were compared, and the influence of inflow and blood oxygen level–dependent (BOLD) effects on the signal variations was assessed with the dual-echo GRE sequences.**

RESULTS: **In 11 of the 12 subjects we found activation in the primary motor cortex with both the GRE and EPI sequences. Active voxels had a significantly higher mean percentage of signal changes with the EPI sequence than with the GRE sequence (EPI: 1% to 6.1%, mean 2.4%; GRE: 1% to 4.5%, mean 1.9%). The EPI sequence was less sensitive to motion artifacts and enabled imaging of a larger brain volume in a shorter time. With a dual-echo sequence we found an increasing contribution of inflow effect with an increasing percentage of signal changes.**

CONCLUSION: **Functional MR imaging of the sensorimotor cortex can be routinely performed at 1.0 T.**

Functional MR imaging, used for visualization and localization of neuronal activity (1–15), is performed mainly on 1.5- to 4.0-T scanners (1–12, 14–19). The increasing demand for functional MR imaging (eg, neurosurgical planning of brain tumor resection) raises the question of whether it can be routinely performed on 1.0-T MR units (13). This capability would expand the accessibility of functional MR imaging to more clinical centers. The signal changes in functional MR imaging caused by blood oxygen level–dependent (BOLD) contrast, typically 1% to 5% at 1.5 T (5), are located in the capillaries of the gray matter of active brain regions and further downstream in the venous system, where the signal variations diminish as the oxyhemoglobin overshoot is increasingly diluted. The size of the signal increase during neuronal activity is related to magnetic field strength. Smaller signal increases are seen at lower field strengths (5, 13, 17–19).

The most common techniques used for functional MR imaging are gradient-echo (GRE) and echo-planar imaging (EPI) (1–19). In this study we compared the functional data acquired with EPI versus GRE sequences to assess the feasibility of functional MR imaging on a 1.0-T MR scanner.

Received August 11, 1997; accepted after revision December 6.

From the Department of Radiology, University Hospital Nijmegen, P.O. Box 9101, 6500 HB Nijmegen, the Netherlands. Address reprint requests to Bas F. W. van der Kallen, MD.

Methods

Functional MR imaging was performed on a standard clinical 1.0-T MR scanner (maximum gradient strength, 20 mT/m; minimal rise time, 0.8 milliseconds) equipped with EPI using a standard circularly polarized head coil. To reduce motion artifacts the subject's head was immobilized in the head coil by using a vacuum pillow and ear pads.

Scout images in three orthogonal projections were acquired to position a midsagittal section (spin-echo sequence: 350/15 [TR/TE], section thickness = 5 mm, matrix = 256 × 256, field of view (FOV) = 230 × 230 mm). Fifteen T1-weighted sections (spin-echo sequence: 500/15, thickness = 5 mm, gap = 0.5 mm, matrix = 256 × 256, FOV = 230 × 230 mm) were positioned parallel to the anterior commissure/posterior commissure (AC/PC) plane. The sections covered the brain from the vertex to approximately 12 mm beneath the AC/PC plane.

Before the functional images were acquired, a global multiple angle projection shim was done to increase the homogeneity of the volume to be imaged.

Functional images were acquired using three sequences: EPI, fast low-angle shot (FLASH), and dual-echo FLASH. The 15 EPI (single-shot EPI free induction decay [$T2^*$] sequence: 4000/66, flip angle = 90°, matrix = 64 × 64, readout band-

width = 780 Hz/pixel, constant phase encoding, and fat suppression) section positions were identical to those on the anatomic reference images. From the 15 anatomic images, we chose the position of the FLASH images to coincide with the sections that included the Ω shape of the central sulcus, known to contain the motor cortex of the hand (12). The FLASH sequence (two sections: 162/46, flip angle = 30°, matrix = 64 × 64, readout bandwidth = 19 Hz/pixel) was acquired in 12 seconds. The dual-echo FLASH sequence (three sections: 150/15, 35; flip angle = 30°, matrix = 128 × 64, readout bandwidth = 65 Hz/pixel) was also acquired in 12 seconds. All functional images had an FOV of 230 × 230 mm, a section thickness of 5 mm, and a section gap of 0.5 mm.

The study included 12 subjects (six men and six women) 21 to 31 years old. All subjects were right-handed according to the Edinburgh Handedness Inventory (20).All subjects performed a hand-motor task for which they were preinstructed to turn a knob with all fingers (and thumb) of their dominant hand in a self-paced manner. The task was performed during two EPI, two FLASH, and one dual-echo FLASH examinations. All examinations were performed during one session lasting 45 to 60 minutes. The order of the examinations was randomized to exclude any order-related effects (eg, habituation, concentration, etc). During the EPI examination, 56 measurements were obtained. The first seven measurements were discarded to ensure that baseline stability of the signal intensity time course was reached. The next 49 measurements were run in a seven off/seven on cycle, resulting in four rest and three activation periods. During the FLASH examinations, 35 measurements were acquired in a five off/five on cycle, again with four rest and three activation periods.

Postprocessing was done on a SunSparc station 20, using the Stimulate functional MR imaging analysis software package (Strupp, "Stimulate: A GUI Based Functional MR Imaging Analysis Software Package" demonstrated at the Second International Conference on Functional Mapping of the Human Brain, Boston, June 1996) and on a Pentium PC with proprietary software. The functional imaging data were viewed in cine mode to scan for head motion. If any motion was apparent, the data were discarded. No motion correction of the images was performed to analyze and compare the original data.

The signal intensity time course of each voxel of the functional imaging data were cross-correlated with a square-wave form with sloped transition periods. For the EPI examinations, the first two images of each on and off period were deleted to account for the lag in signal intensity increase after the start of the motor task (90% of signal intensity increase at 5 to 8 seconds) (5). This was not done for the FLASH examinations, because the lag in signal intensity increase is shorter than the 12-second acquisition period of one image volume. Consequently, in both the EPI and the FLASH examinations, 35 images were used in the cross-correlation analysis. In the EPI sequence, the imaging data were rearranged so that only the two sections of the EPI examination that were identical to the sections in the FLASH examination were used in the analysis; thus, both the FLASH and EPI examinations had identical data arrangements in the cross-correlation analysis. The functional data were analyzed with an empirically chosen cross-correlation threshold of $r > 0.5$. Additionally, the voxels passing the cross-correlation threshold were only displayed when located in a cluster of two or more to remove noise artifacts (16). The signal-intensity characteristics of the voxels in the two analyzed sections passing the postprocessing criteria were used to assess the difference between EPI and FLASH at 1.0 T. The percentage of signal increase from baseline (ΔS) was calculated by dividing the mean signal intensity difference of a voxel between rest and activation by the mean baseline signal intensity. The amount of pixels passing the postprocessing criteria, the mean ΔS, and the maximum ΔS were tabulated. The data from all active voxels in the two sections and/or the data from a region of interest (ROI) covering the left sensorimotor cortex were used for further comparison. In each subject, the boundaries of the sensorimotor cortex ROI were drawn (before postprocessing) anteriorly through the middle of the precentral gyrus, posteriorly through the middle of the postcentral gyrus, and laterally and medially through the borders of the central sulcus. The mean center of mass and the standard deviation (SD) during an examination (35 sequence measurements) were calculated to compare the residual motion of EPI and FLASH. Of the obtained data, the significance of the difference between the EPI and FLASH examinations was tested using an unpaired two-tailed Student's *t*-test.

For the dual-echo sequence, we assessed and compared the mean number of active voxels and the mean and maximum ΔS in the sensorimotor cortex ROI for the TEs of 15 and 35. Additionally, we obtained the influence of inflow and BOLD contrast on the signal-intensity changes of the voxels passing the postprocessing criteria. The voxels active in the TE = 15 images (inflow) were overlaid on the voxels active in the TE = 35 images (inflow + BOLD). Subsequently, we assessed the ΔS of each overlapping voxel (active in TE = 15 and TE = 35 images) and of each nonoverlapping voxel (only active with TE = 35). The ΔS of the overlapping and the nonoverlapping voxels was tabulated in 10 bins of equal width from 1% to 5%. Thus, a frequency distribution of ΔS for the overlapping (inflow + BOLD) and nonoverlapping (BOLD) voxels was acquired. The difference in the frequency distribution between overlapping and nonoverlapping voxels was tested using the nonparametric Mann-Whitney test.

Results

Of the 12 subjects scanned in this study, the results for one subject had to be discarded, as she repeatedly fell asleep during the examination, which resulted in head motion and inconsistent task performance. In two other subjects, the dual-echo examinations showed gross motion artifacts, causing these data to be excluded from further analysis. Thus, 11 subjects successfully performed the EPI and FLASH experiments, and nine subjects successfully completed the dual-echo experiments.

The cerebral activity on FLASH and EPI examinations resulting from the execution of the motor task in a representative subject is shown in Figure 1. The voxels passing the postprocessing criteria were color coded (ΔS: red ↔ yellow = 1% ↔ 5%) and overlaid on the anatomic reference images. Activation of the contralateral sensorimotor cortex was seen in all subjects, regardless of the imaging sequence used. The extent of the activation of other brain regions during performance of the motor task was consistent within subjects. Yet, between subjects, there was a variation in the activation of other brain regions, indicating possible intersubject variability in the utilization of different brain regions in the execution of a self-paced motor task. Variable activation was seen in the ipsilateral sensorimotor cortex, the premotor cortex, the supplementary motor area, and the parietal cortex. In the additional sections acquired with the EPI sequence (Fig 2), activation was also seen in the cingulate gyrus, the ventral opercular premotor area, and the thalamus. The functional MR imaging data were overlaid on the original EPI images. These images showed apparent distortions around air-tissue-bone interfaces with EPI at 1.0 T. The functional MR imaging data of the sections through the primary

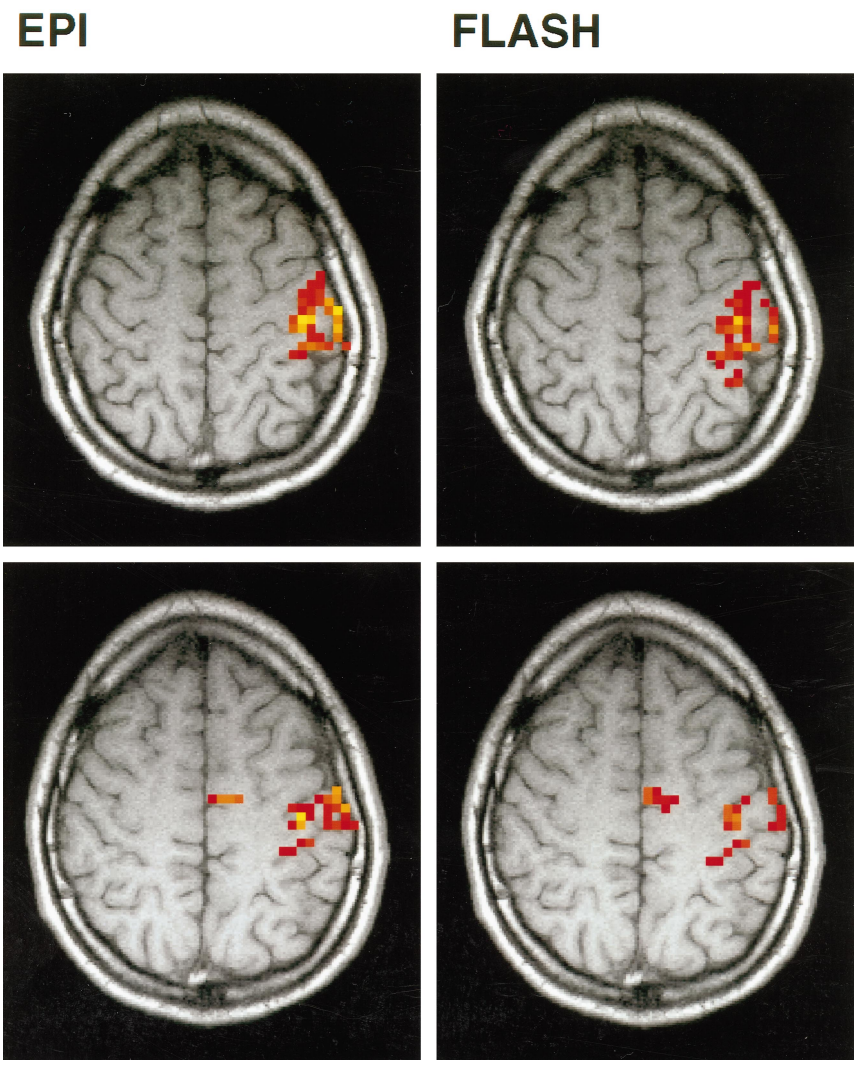

FIG 1. Functional images (two sections) of EPI (4000/66/1) and FLASH (162/46/1) sequences in a representative subject. Voxels passing the postprocessing criteria are color coded (ΔS: red ↔ yellow = 1% ↔ 5%) and overlaid on anatomic spin-echo reference images. During the performance of a motor task, similar activation is seen in the contralateral sensorimotor cortex, the parietal cortex, and the supplementary motor area on both the EPI and FLASH examinations.

motor cortex used to compare EPI with GRE were not markedly distorted. The activation pattern and location were similar for the FLASH and EPI examinations.

Results of the EPI and FLASH Sequences

Figure 3 shows the average signal time course for the series of 35 EPI and FLASH images in the left sensorimotor cortex of the subject displayed in Figure 1. The signal intensity increases seen during the task performance were greater with the EPI sequence. Figure 4 shows the mean ΔS for the EPI and FLASH examinations for the 11 subjects (number of examinations for each sequence = 22) in the left sensorimotor cortex and for the total number of active voxels in the two sections. A significantly greater mean ΔS was seen for the EPI sequence than for the FLASH sequence ($EPI_{sensorimotor\ cortex} = 2.4$, $FLASH_{sensorimotor\ cortex} = 1.9$; $P < .009$; $EPI_{total} = 2.2$, $FLASH_{total} = 1.8$; $P < .009$). Also, the maximum ΔS was markedly greater for the EPI than for the FLASH examinations, as shown in Figure 5 ($EPI_{sensorimotor\ cortex} = 5.8$, $FLASH_{sensorimotor\ cortex} = 4.0$; $P < .04$; $EPI_{total} = 6.1$, $FLASH_{total} = 4.5$; $P < .01$]).

There was no significant difference in the amount of active voxels in the left sensorimotor cortex or in the total number of active voxels between the FLASH and EPI examinations: mean (SEM) for $EPI_{sensorimotor\ cortex} = 30$ (2.8); for $FLASH_{sensorimotor\ cortex} = 23$ (2.3); for $EPI_{total} = 72$ (8.9); for $FLASH_{total} = 50$ (7.8).

The center of mass movement during the functional MR imaging examinations was reflected by the SD from the mean center of mass in the *x* (horizontal) and *y* (vertical) directions. The SD was markedly higher during the FLASH sequences (mean SD: EPI-$x = 0.013$, FLASH-$x = 0.034$, $P < .0001$); EPI-$y = 0.016$, FLASH-$y = 0.027$, $P < .015$).

Results of the Dual-Echo Sequence

The number of active voxels in the left sensorimotor cortex in the three sections, obtained at TEs of 15 and 35 for the nine dual-echo examinations, significantly increased with a TE of 35: mean (SEM) = 78 (17.9) in contrast to 16 (5.4) for a TE of 15 ($P < .009$). Figure 6 displays the mean and maximum ΔS at TEs of 15 and 35 for the same two sections as in the EPI and FLASH examinations. There was no significant

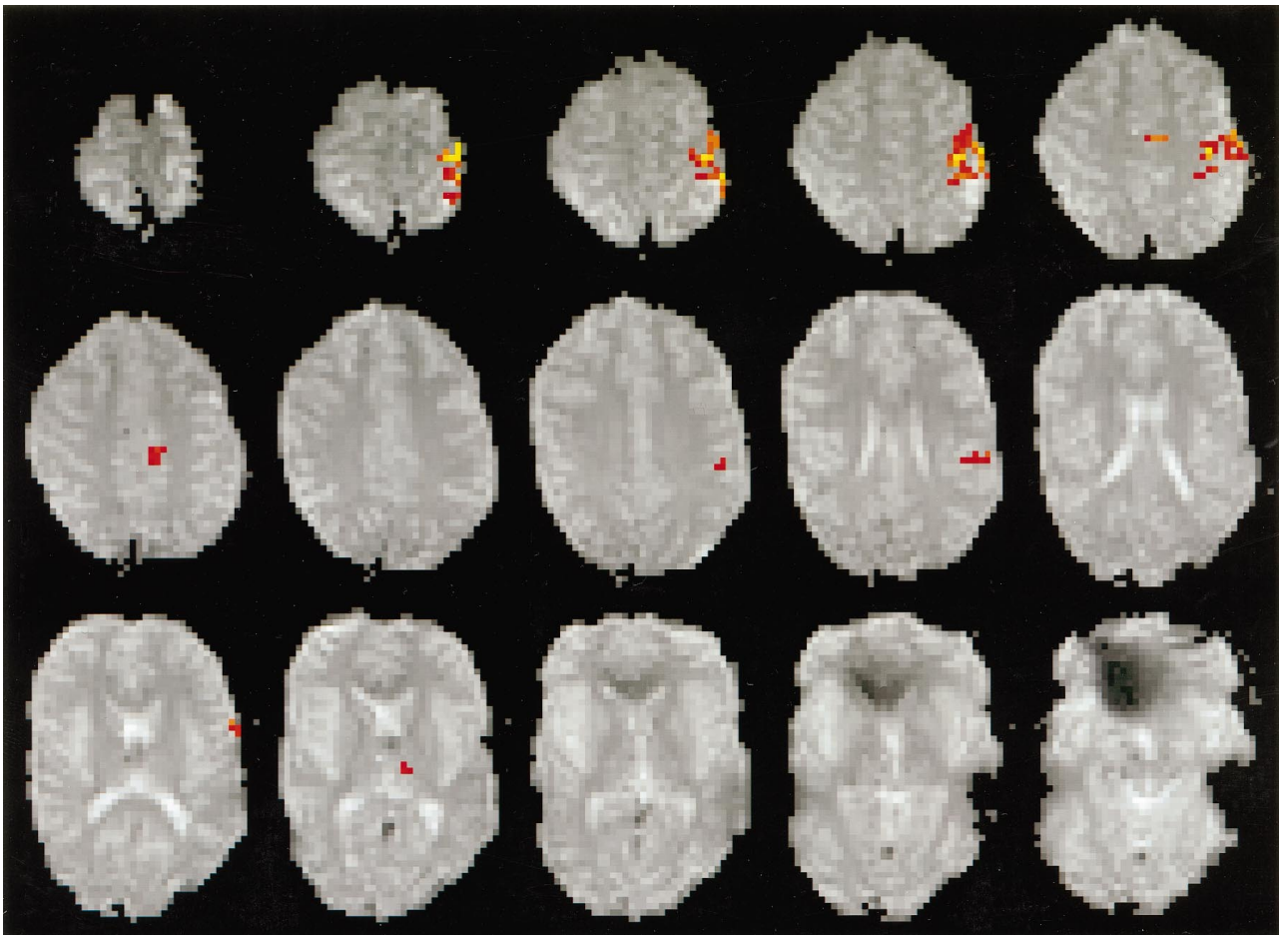

FIG 2. All 15 sections of the EPI sequence (4000/66/1) of the subject in Figure 1. Active voxels are color coded (ΔS: red ↔ yellow = 1% ↔ 5%). In addition to that noted in Figure 1, activation is also seen in the cingulate gyrus, the ventral opercular premotor area, and the thalamus. In the EPI images, apparent distortions are seen around air-tissue-bone interfaces. The sections through the primary motor cortex used to compare EPI with GRE had no evident image distortions.

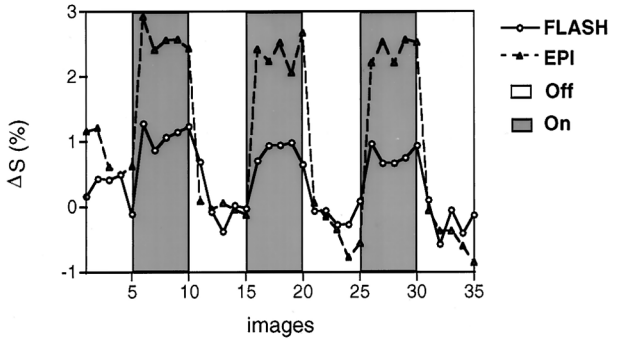

FIG 3. Average signal time course of the voxels passing the postprocessing criteria for the series of 35 EPI and FLASH images the left sensorimotor cortex (subject in Fig 1). The signal intensity in the sensorimotor cortex increased during the performance of the motor task. Greater signal variations were seen with the EPI sequence. $\Delta S\ (\%) = S_{image} - S_{baseline\ mean}/S_{baseline\ mean} \times 100$.

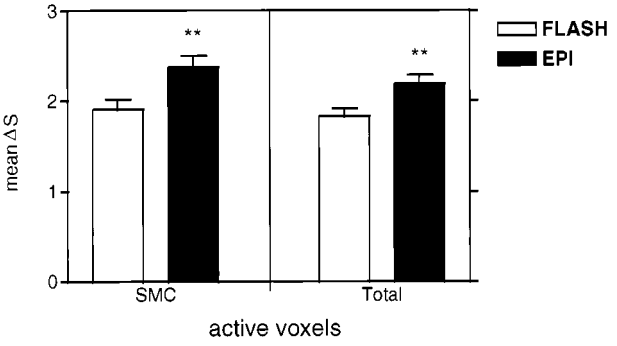

FIG 4. Mean ΔS for the EPI and FLASH examinations of the 11 subjects (22 examinations for each sequence). The mean ΔS of the active voxels in the left sensorimotor cortex and also for the total number of active voxels in the two sections analyzed are displayed. ($^{**}P < .01$.)

difference between the mean ΔS with TEs of 15 and 35 (mean ΔS for TE of 15 = 1.7; for TE of 35 = 1.9). Yet there was a marked increase in the maximum ΔS when the TE was lengthened from 15 to 35 (maximum ΔS for TE of 15 = 2.3; for TE of 35 = 3.9; $P < .016$). Figure 7 displays the frequency distribution of the ΔS of the overlapping (active during TE = 15 and TE = 35 [n = 131]) and nonoverlapping (only active during TE = 35 [n = 578]) voxels. The distribution of the overlapping voxels (BOLD + inflow) was significantly shifted to the right as compared with the nonoverlapping voxels (BOLD): mean ΔS (SEM) for nonoverlapping voxels = 1.9 (0.03); for overlapping voxels = 2.5 (0.09); $P < .0001$. Thus, as the ΔS increased, a greater contribution of the inflow effect

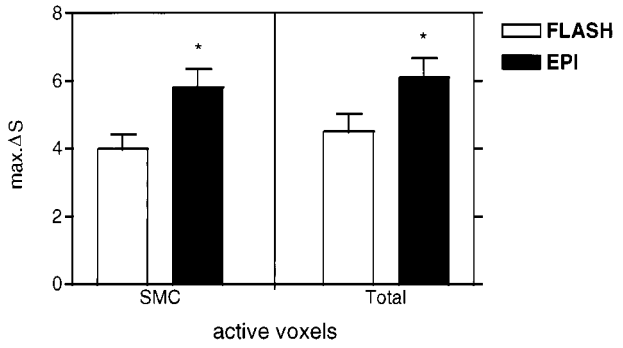

FIG 5. Maximum ΔS for the EPI and FLASH examinations in the left sensorimotor cortex and for the total number of active voxels in the two sections analyzed. (*$P < .05$.)

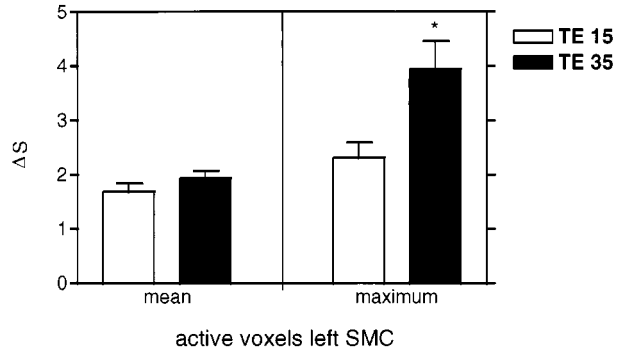

FIG 6. Mean and maximum ΔS at TEs of 15 and 35 (dual-echo FLASH). (*$P < .05$.)

was seen. The nonoverlapping (BOLD) voxels were situated mainly between the 1% to 2% ΔS range, as shown in Figure 8. The activation in the left sensorimotor cortex with a TE of 15, a TE of 35, and the overlapping voxels was overlaid on a corresponding TE 35 FLASH image for a representative subject (Fig 8). The overlapping voxels had a high ΔS, demonstrating that the inflow effect contributes mainly to the voxels with greater signal variations.

The dual-echo sequence was also used to calculate the $T2^*$ of gray matter. Using the equation

$$1) \qquad T2^* = (TE_B - TE_A)/\ln(S_A/S_B),$$

where TE_A is 15, TE_B is 35, and S_A and S_B are the signal intensities of gray matter at echo times of 15 and 35, respectively (21), resulted in a $T2^*$ of 82 milliseconds.

Discussion

In this study we compared the functional data of an EPI sequence with that of a GRE sequence in healthy volunteers to assess which sequence performs best at 1.0 T (13). The major disadvantage of using GRE sequences for functional MR imaging is the long acquisition time (13, 18). The acquisition time for one section is of such length that it necessitates a compromise between the number of sections imaged, the TE, the TR, and the size of the matrix. Conversely, EPI enables multisection whole-brain imaging in 2 to

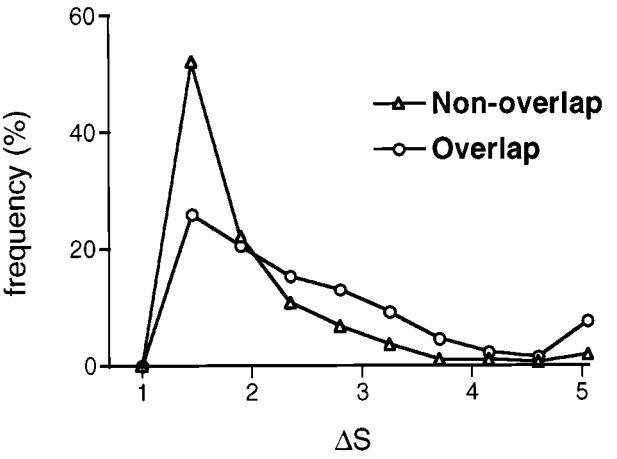

FIG 7. Frequency distribution of the ΔS of the overlapping (active during TEs of 15 and 35, n = 131) and nonoverlapping (only active during TE of 35, n = 578) voxels. The ΔS of the overlapping voxels is a combination of BOLD contrast and inflow effect, whereas the ΔS of the nonoverlapping pixels is mainly due to the BOLD contrast.

5 seconds, even with a longer TE (5). For the FLASH sequence, two sections were chosen to cover a relatively large portion of the sensorimotor cortex of the hand, making the statistical comparison of this region between the sequences stronger. Yet, not all the hand sensorimotor cortex was enclosed, as was seen by activation in the other EPI sections not covered by the FLASH sequence. Owing to the dissimilarity in the acquisition principles and the sequence designs of EPI and GRE imaging, different imaging parameters had to be used. The sequences differed in TE, TR, and flip angle. The image position, matrix size, FOV, section thickness, and gap of both sequences were kept identical. We optimized the FLASH sequence to have an acceptable acquisition time (TE, TR, number of sections) and relative insensitivity to inflow effects (TR and flip angle). The EPI sequence did not allow for a shorter TE than 66 milliseconds, and a longer TE for the FLASH sequence (46 milliseconds) would have resulted in a longer acquisition time. The active voxels in the FLASH sequence had a ΔS range of 1% to 4.5% (mean, 1.9%); for the EPI sequence, the range was 1% to 6.1% (mean, 2.4%). For the gray matter of the sensorimotor cortex, we calculated a $T2^*$ value of 82 milliseconds at 1.0 T. Therefore, the optimal TE for BOLD contrast was around 82 milliseconds. The longer TE of the EPI sequence makes it sensitive to BOLD contrast, which is why the mean ΔS of the EPI sequence was higher than that of the FLASH sequence. Yet, the mean ΔS of the GRE sequences did not increase significantly when the TE was raised from 15 to 35 to 46 milliseconds. Therefore, it is likely that other factors were also of influence.

Other factors that influence the ΔS are the inflow effect and artifacts, such as from subject motion or physiological (cardiac and pulmonary) motion. The dual-echo sequence showed a relative increase of the inflow effect in voxels with a larger ΔS. Therefore, the higher maximum and mean ΔS of the EPI sequence are possibly a consequence of a greater con-

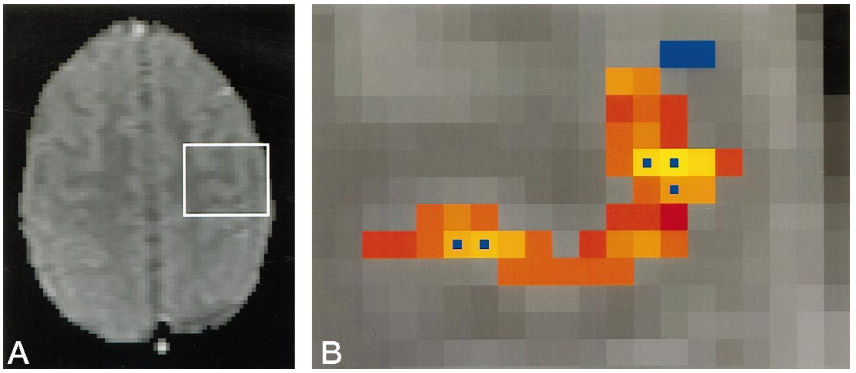

FIG 8. Overlaid on a corresponding dual-echo FLASH sequence (150/15, 35/1) and zoomed in (*white box*) (*A*) is the activation in the left sensorimotor cortex (*B*) for a representative subject. The voxels active with a TE of 15 appear in blue (inflow); those active with a TE of 35 are color coded as ΔS: red ↔ yellow = 1% ↔ 5%. Overlapping voxels are color coded for TE = 35 with an additional central blue pixel (TE = 15). The overlapping voxels have a high ΔS, demonstrating that the inflow effect contributes mainly to the voxels with greater signal variations.

tribution of inflow effect to the signal increase during neuronal activity than occurs with the FLASH sequence. Although a flip angle of 90° was used in the EPI sequence, the sequence TR of 4 seconds was sufficiently long to minimize the contribution of the inflow effect to ΔS (17, 22). Moreover, the dual-echo sequence showed that the signal variations in the FLASH sequence were also partly due to inflow effect. Of the active voxels, the ΔS of the BOLD voxels was mainly in the lower range of the signal variations (1% to 2%). Still, the BOLD contrast accounted for most of the total number of voxels passing the postprocessing criteria. The low ΔS makes functional MR imaging at 1.0 T very sensitive to artifacts. The sensitivity to motion artifacts is less for EPI than for GRE imaging as a consequence of the faster image acquisition time. Accordingly, we observed a significantly smaller center of mass movement in the EPI sequences. This also accounts for the greater ΔS with EPI, as the cross-correlation analysis is influenced by motion artifacts (5, 9).

In our healthy volunteers, activation of the sensorimotor cortex was seen in all subjects on both FLASH and EPI sequences. Thus, visualization of the sensorimotor cortex is highly reproducible at 1.0 T. The activation of other brain regions was more variable, and further studies are necessary to explain whether these variations are a consequence of individual physiological differences or inherent scanner variations.

Conclusion

Comparison of the results of EPI and FLASH examinations of the sensorimotor cortex showed that the EPI sequence at 1.0 T had a higher percentage of signal change than did the FLASH sequence, with a similar amount of activation in the sensorimotor cortex. Also, the EPI sequence was less sensitive to motion artifacts and enabled the acquisition of multiple sections showing the whole brain. We conclude that it is feasible to perform functional MR imaging of the primary motor area at 1.0 T, preferably using an EPI sequence.

References

1. Ogawa S, Tank DW, Menon RS, et al. **Intrinsic signal changes accompanying sensory stimulation: functional brain mapping with magnetic resonance imaging.** *Proc Natl Acad Sci U S A* 1992;89:5951–5955
2. Ogawa S, Menon RS, Tank DW, et al. **Functional brain mapping by blood oxygenation level-dependent contrast magnetic resonance imaging: a comparison of signal characteristics with a biophysical model.** *Biophys J* 1993;64:803–812
3. Belliveau JW, Kennedy DN, McKinstry RC, et al. **Functional mapping of the human visual cortex by magnetic resonance imaging.** *Science* 1991;254:716–719
4. Bandettini PA, Wong EC, Hincks PS, Tikofsky RS, Hyde JS. **Time course EPI of human brain function during task activation.** *Magn Reson Med* 1992;25:390–397
5. Bandettini PA, Jesmanowicz A, Wong EC, Hyde JS. **Processing strategies for time course data sets in functional MRI of the human brain.** *Magn Reson Med* 1993;30:161–173
6. Rao SM, Binder JR, Bandettini PA, et al. **Functional magnetic resonance imaging of complex human movements.** *Neurology* 1993; 43:2311–2318
7. Kim S-G, Ashe J, Georgopoulos AP, et al. **Functional imaging of human motor cortex at high magnetic field.** *J Neurophysiol* 1993; 69:297–302
8. Frahm J, Bruhn H, Merboldt K, Hanicke WLF. **Dynamic MR imaging of human brain oxygenation during rest and photic stimulation.** *J Magn Reson Imaging* 1992;2:501–505
9. DeYoe EA, Bandettini P, Neitz J, Miller D, Winans P. **Functional magnetic resonance imaging (fMRI) of the human brain.** *J Neurosci Meth* 1994;54:171–187
10. Kwong KK, Belliveau JW, Chesler DA, et al. **Dynamic magnetic resonance imaging of human brain activity during primary sensory stimulation.** *Proc Natl Acad Sci U S A* 1992;89:5675–5679
11. Hammeke TA, Yetkin FZ, Mueller WM, et al. **Functional magnetic resonance imaging of somatosensory stimulation.** *Neurosurgery* 1994;35:677–681
12. Rumeau C, Tzourio N, Murayama N, et al. **Location of hand function in the sensorimotor cortex: MR and functional correlation.** *AJNR Am J Neuroradiol* 1994;14:567–572
13. Santosh CG, Rimmington JE, Best JJK. **Functional magnetic resonance imaging at 1T: motor cortex, supplementary motor area and visual cortex activation.** *Br J Radiol* 1995;68:369–374
14. Moser E, Teichtmeister C, Diemling M. **Reproducibility and postprocessing of gradient-echo functional MRI to improve localization of brain activity in the human visual cortex.** *Magn Reson Imaging* 1996;14:567–579
15. Krüger G, Kleinschmidt A, Frahm J. **Dynamic MRI sensitized to cerebral blood oxygenation and flow during sustained activation of human visual cortex.** *Magn Reson Med* 1996;35:797–800
16. Forman SD, Cohen JD, Fitzgerald M, Eddy WF, Minun MA, Noll DC. **Improved assessment of significant activation in functional magnetic resonance imaging (fMRI): use of a cluster-size threshold.** *Magn Reson Med* 1995;33:636–647
17. Kim S-G, Hu X, Adriany G, Uğurbil K. **Fast interleaved echo-planar imaging with navigator: high resolution anatomic and functional images at 4 Tesla.** *Magn Reson Med* 1996;35:895–902
18. Kim S-G, Hendrich K, Hu X, Merkle H, Uğurbil K. **Potential pitfalls of functional MRI using conventional gradient-recalled echo techniques.** *NMR Biomed* 1994;7:69–74
19. Duyn JH, Moonen CTW, van Yperen GH, de Boer RW, Luyten PR. **Inflow versus deoxyhemoglobin effects in BOLD functional MRI using gradient echoes at 1.5 T.** *NMR Biomed* 1994;7:83–88
20. Oldfield RC. **The assessment and analysis of handedness: the Edinburgh inventory.** *Neuropsychologia* 1971;9:97–113
21. Hajnal JV, Roberts I, ilson J, et al. **Effect of profound ischeamia on human muscle: MRI, phosphorus MRS and near-infrared studies.** *NMR Biomed* 1996;9:305–314
22. Kim SG, Uğurbil K. **Comparison of blood oxygenation and cerebral blood flow effects in fMRI: estimation of relative oxygen consumption change.** *Magn Reson Med* 1997;38:59–65